*Article*

# Quantitative Analysis of Chlorogenic Acid during Coffee Roasting via Raman Spectroscopy

Deborah Herdt [1,*], Tobias Teumer [2], Shaun Paul Keck [3,†], Thomas Kunz [4], Victoria Schiwek [4], Sarah Kühnemuth [4], Frank-Jürgen Methner [4] and Matthias Rädle [1]

[1] CeMOS Research and Transfer Center, Mannheim University of Applied Sciences, 68163 Mannheim, Germany; m.raedle@hs-mannheim.de
[2] SAT Anlagentechnik GmbH, 25578 Daegeling, Germany; tobias.teumer@sat-sterling.com
[3] Lummus Novolen Technology GmbH, 68165 Mannheim, Germany; shaun.keck@lummustech.com
[4] Institute of Food Technology and Food Chemistry, Department of Brewing and Beverage Technology, Technical University, 13355 Berlin, Germany; thomas.kunz@tu-berlin.de (T.K.); victoria.schiwek@tu-berlin.de (V.S.); sarah.kuehnemuth@tu-berlin.de (S.K.); frank-juergen.methner@tu-berlin.de (F.-J.M.)
* Correspondence: d.herdt@hs-mannheim.de
† The author is a Process Technology Expert for Lummus Novolen Technology. The below text reflects solely the opinion of the author and not the opinion of Lummus Novolen Technology.

**Abstract:** Tracking coffee roasting at an industrial scale for quality control is challenging. Bean color is a practical gauge for monitoring and regulating the process but only occurs before and after the process. This study highlights the feasibility of monitoring the process throughout using Raman spectroscopy. Strecker degradation and the Maillard reaction contribute to various aromatic compounds that can serve as markers in quality monitoring. Among these are chlorogenic acids (CGAs), recognized as pivotal factors determining the desired aroma. Here, drum and fluidized bed roaster processes were monitored, capitalizing on the chemical alterations induced by high temperatures (140–200 °C), particularly through the Maillard reaction. These chemical changes manifest in the scattered light signal. For real-time monitoring, Raman spectra were taken every 10 ms in selected ranges, with an average calculated every second. Utilizing a calibration matrix from a High-Pressure Liquid Chromatography (HPLC) method, CGA concentration becomes the control variable for assessing roasting progress. This study reveals the potential of Raman spectroscopy for tracking CGA during roasting. It establishes a correlation between inelastic scattered light and CGA validated through laboratory measurements and fixed roasting conditions, resulting in a theoretical CGA concentration that can be used as a process termination criterion.

**Keywords:** Raman spectroscopy; chlorogenic acid; coffee roasting; degree of roasting; quality control; HPLC-DAD

## 1. Introduction

Coffee roasting is both a science and an art, transforming raw green coffee beans into the aromatic and flavorful beans that perk up mornings and are subject to scientific research worldwide. This pivotal stage in coffee production holds the key to unlocking the spectrum of flavors, aromas, and complexities inherent in different products [1]. Controlled heat transfer induces a sequence of chemical reactions within the beans, each phase timed to extract the desired characteristics for the specific coffee blend, from the initial moisture evaporation and the Maillard reaction's progression to the balance between caramelization and the pyrolysis of organic compounds. The application of heat triggers a cascade of reactions within the coffee beans, altering their composition and character [1]. This journey begins with the raw green coffee beans—each variety possessing distinct flavors and attributes. The beans undergo a profound transformation from their raw green state to a

spectrum of browns, each shade representing a different depth of flavor [2,3]. Temperature, duration, and the roasting environment play pivotal roles in the roasting process. First, moisture within the beans evaporates, leading to an audible 'first crack' [4,5]. Sugars caramelize, organic acids break down, and the Maillard reaction is initiated, with amino acids reacting with reducing sugars [6–9]. Initially, the sugars undergo dehydration and fragmentation, forming reactive carbonyl groups. These then interact with the amino acids, leading to the formation of a wide range of flavorful compounds. The Maillard reaction is not a single reaction but rather a cascade of multiple reactions involving hundreds of different compounds [6,10]. These reactions result in the formation of various flavorful and aromatic molecules such as pyrazines, furans, and thiazoles, contributing to the rich taste and appealing aroma of roasted foods [11–13]. The reaction does not occur instantly but progresses as the temperature continues to rise. Different temperatures can produce different flavors and colors. At lower temperatures, the reaction might proceed slowly, resulting in lighter flavors and colors. However, higher temperatures can lead to faster and more intense reactions, producing darker colors and more complex flavors [8,12]. As amino acids and reducing sugars engage in the Maillard reaction, generating a vast number of aromatic compounds and flavors, a subset of amino acids undergoes a parallel transformation known as the Strecker degradation. This pathway represents a complementary reaction in flavor development, where amino acids are transformed into various volatile compounds [14], amplifying the sensory appeal of roasted foods [15]. In the context of coffee roasting, the Strecker degradation occurs when amino acids, present in the raw bean, decompose due to the high temperatures involved. When subjected to heat, these amino acids can undergo a series of chemical reactions involving $\alpha$-dicarbonyl compounds, such as reducing sugars or their breakdown products, which are also generated during roasting [16]. The process begins with the condensation of $\alpha$-dicarbonyl compounds with amino acids, leading to the formation of intermediates known as $\alpha$-amino carbonyl compounds [17]. Previously, studies have shown a large number of intermediates and substances that can be used to identify the progress of browning, the antioxidant and pro-oxidant activity or formation of 1,2-dicarbonyl compounds [18,19]. Intermediates are highly reactive and undergo further transformations, including decarboxylation and deamination, resulting in the production of a diverse array of volatile compounds [14,20]. These volatile compounds, including aldehydes, ketones, and heterocyclic compounds, contribute significantly to the aroma and flavor profile of roasted coffee. Rusinek et al. [21] demonstrated that different roasting levels generate varying levels of phenolic compounds, caffeine, and tocopherols, with significant differentiation in the coffee bean's chemical properties. The extent and variety of compounds formed through the Strecker degradation depend on several factors, including the types and concentrations of amino acids present, roasting temperature and duration, and the moisture content of the coffee variety. Understanding the Strecker degradation during the roasting process not only explains the formation of key aroma compounds but also provides insights into optimizing roasting conditions for the development of specific and desirable sensory attributes [8,9,11,15,17,22,23].

The Strecker degradation as well as the Maillard reaction not only contribute to the diverse array of aromatic compounds but also serve as critical markers in quality monitoring within the roasting process. Some of these components are chlorogenic acids (CGAs), which are known to be quality-determining factors for the desired coffee aroma [24,25]. The monitoring and understanding of chemical reactions become pivotal. By tracking the progression of those pathways, roasters gain insight into the evolving flavor profile, enabling precise control and optimization of roasting conditions [23]. The integration of online monitoring of the chemical composition of coffee forms one possibility of quality control, ensuring that each batch of roasted coffee obtains the desired aroma complexity and color. In the production of roasted products, current quality monitoring relies heavily on assessing color as an indirect quality indicator [26]. However, this approach exhibits a weak correlation with the ideal flavor quality. Professional roasters, particularly those focusing on small, high-quality batches, often rely on personal sensory evaluation to guide their

control variables during the roasting process [27]. This evaluation heavily draws upon the roaster's expertise and initial assessments of the specific roasting chamber used. However, relying on sensory evaluations, such as odor or visual cues, demands extensive training and experience, which, in turn, means that these procedures cannot be automatable. At present, there is no standardized market-available measurement specifically designed for roasting coffee that adequately addresses quality assurance, especially concerning sensory characteristics [26,27].

In industrial applications, the color of coffee beans becomes a practical metric for monitoring and controlling the roasting process [28]. However, this metric is commonly compared before and after roasting, rather than during the process itself. Consequently, many roasters still rely on routine process flows and controlling the oven temperature. The roasting process itself is influenced by factors such as water content, grain size, geographical origin, vintage, and the variety of coffee beans. The two main coffee bean varieties, robusta and arabica, exhibit distinct roasting behaviors. Additionally, uneven roasting, marked by substantial temperature variations within the bean, results in some areas being under-roasted while others are over-roasted [28]. Achieving standardization therefore is challenging, as these influences persist independently of roaster type or filling degree [26,29–31].

Transitioning from the challenges of relying on color comparison and routine process flows in coffee roasting, there is a pressing need for advanced methodologies that overcome these limitations. The integration of infrared (IR) spectroscopy has emerged as one possible approach in contrast to traditional analytical methods, offering faster analyses and eliminating the need for extensive sample pretreatment [32–34]. In coffee roasting, especially near-infrared (NIR) spectroscopy has proven successful in predicting crucial quality parameters like color [33,35,36], determining the roasting degree [37], and chemical changes [38,39]. Mid-infrared (MIR) spectroscopy has been explored with offline techniques for quality control [40–43] or even to discriminate coffee variants [44].

The comprehensive review by Munyendo et al. [45] summarizes recent advancements in the application of various spectroscopic techniques, including mid-infrared, near-infrared, Raman, and fluorescence spectroscopy, for coffee analysis. Munyendo et al. indicated that, while robust prediction models show that spectroscopic methods can evaluate coffee across the production process, Raman and fluorescence spectroscopy remain underexplored despite their significant potential for providing valuable information. While infrared spectroscopy has demonstrated its value in offering quality control, Raman spectroscopy presents an additional possibility. Exploring the molecular realm, Raman spectroscopy operates on the principle of inelastic scattering when monochromatic light interacts with a molecule's electron shell (Stokes Raman Scattering). Unlike infrared (IR) spectroscopy, where the excited vibration matches the photon frequency, Raman spectroscopy's molecular vibration indirectly depends on the excitation radiation wavelength. A vast majority of irradiated light (approximately 99.99%) undergoes elastic scattering (Rayleigh Scattering), while a fraction allows valence electrons to enter a virtual excited state. The Stokes lines, indicating the red-shifted emitted photons, result from energy absorption, representing a lower frequency or longer wavelength. The energy difference is termed the 'Raman shift', with the shift's origin aligning with the excitation wavelength. Generally, quantitative analyses are feasible with Raman spectroscopy, as the intensity of the bands directly correlates with the analyte concentration in the materials [46].

The conventional Raman spectrometer design matches the Czerny–Turner arrangement. It consists of an entrance slit, a collimating mirror or grating, a diffraction grating, and a focusing mirror. The entrance slit allows light into the system, which is then collimated, dispersed by the diffraction grating, and focused onto a detector by the focusing mirror. This arrangement efficiently separates and detects different wavelengths, making it a common design in Raman spectrometers, for precise spectral analysis [47].

The pioneering study by Rubayiza et al. [48] utilized Fourier-transform (FT) Raman spectroscopy for discriminating between botanical species of both green and roasted coffees, specifically examining the lipid fraction in various coffee samples. Visual analysis of the

Raman spectra revealed discernible differences in the mid-wavenumbers region. Raman spectroscopy was also applied to introduce a coffee classifier that utilizes surface-enhanced Raman spectroscopy (SERS), feature extraction, and machine learning, capitalizing on the signal enhancement provided by SERS substrates to detect dilute molecules in coffee [49]. Luna et al. [50] explores the application of chemometric methods in classifying clonal varieties of green coffee with Raman spectroscopy and direct sample analysis. Another study [51] used visible micro Raman spectroscopy in conjunction with principal component analysis (PCA) as a potent technique for rapidly distinguishing between the Arabica and Robusta coffee species, relying on their CGA and lipid contents.

Drawing from these investigations, the application of Raman spectroscopy emerges as a promising tool for monitoring roasting processes, enabling the assessment of roasting aromas and the utilization of coffee constituents to establish termination criteria. Consequently, Raman measurements were conducted in this study to construct a coffee roasting matrix. The findings demonstrate the successful transferability of these measurements to monitor roasting on both drum and fluidized bed roasters. This allows the establishment of a time-dependent and quantitative actuator or roast break criterion.

## 2. Materials and Methods

The raw material, washed green *Coffea arabica* of the Columbia Excelso variety, was supplied by Beans of Joy (Dossenheim, Germany). Multiple roasting trials were conducted to achieve uniform roasting of coffee beans at a consistent temperature and duration in a fluidized bed roaster. These trials served as a benchmark for comparing real-time roasting processes conducted in a drum roaster.

### 2.1. Reference Measurement Roasting

The coffee beans underwent roasting in a laboratory fluidized bed roaster (NEXUS 20, Alfred Nolte, Reinbek, Germany) under atmospheric pressure, as depicted in Figure 1.



**Figure 1.** Fluidized bed roaster NEXUS 20 (Alfred Nolte, Reinbek, Germany).

The fluidized bed roaster ensures a continuous and uniform heat flow, facilitating even roasting of the coffee beans. The air convection maintains a consistent heat transfer rate, making these roasts ideal reference samples for subsequent analysis. To maintain temperature stability during sampling, the roasts were promptly halted after the designated sampling period and promptly cooled by the radiator. Each sampling session involved loading a fresh batch of 1 kg green coffee beans into the roaster. Sampling times were

chosen based on temperature considerations and maintained approximately constant (refer to Table 1). In total, 37 samples were collected along with an additional unroasted sample to facilitate further analysis.

**Table 1.** Roasting test series with temperature and time specification of coffee reference samples.

| Roasting Temperature (°C) | Roasting Time (s) |
| --- | --- |
| 140 | 0, 300, 600, 1200, 1500, 1800, 2100, 2400, 2700, 3000 |
| 160 | 0, 300, 600, 1200, 1500, 1800, 2100, 2400, 2700, 3000 |
| 180 | 0, 240, 480, 720, 960, 1200, 1440, 1680, 1920, 2160 |
| 200 | 0, 180, 360, 540, 720, 900, 1260, 1440, 1620 |

The reference measurements involved fixing the probe head (1 in Figure 2) using a stand (2). The ground coffee sample was placed in a sample container (3) positioned under the probe head, and an even surface was achieved using a tamper. The distance (d) between the probe head and the surface of the filled sample was maintained at 35 mm. Measurement time was set to 10 ms. Each sample underwent fivefold determination. Therefore, for every roasting temperature and time, the sample container was filled five times with freshly ground coffee using a Krups Burr Grinder (Art.no.GVX242, Frankfurt am Main, Germany) set to the finest grinding setting. The average Feret diameter of the ground coffee particles was 760 μm.



(**a**)                                    (**b**)
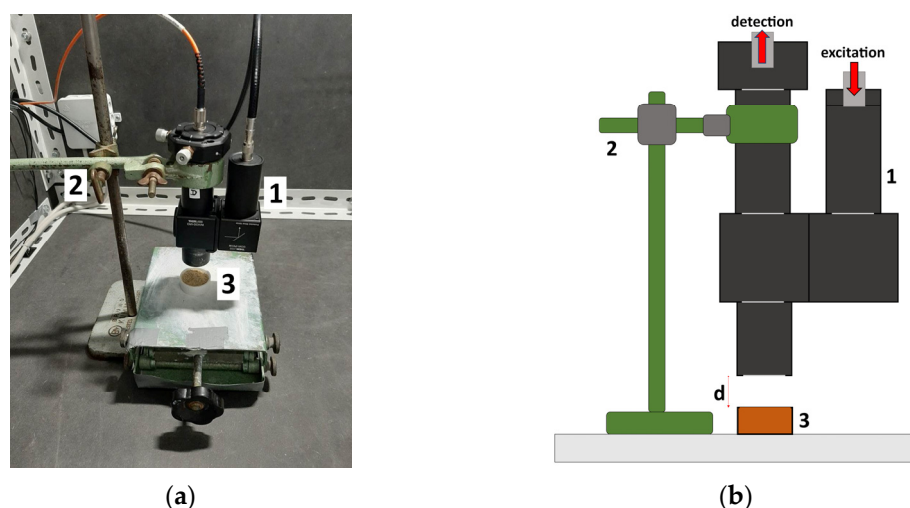
**Figure 2.** Spectroscopic measurements conducted with the probe head in the (**a**) laboratory setup and (**b**) schematic representation showing the probe head (1), stand (2), and sample container holding grounded coffee (3).

### 2.2. Online Measurement Roasting

For each roasting cycle, 500 g of green, unroasted beans was roasted in an Oz macchina drum roaster, powered by gas (Oztrade Ltd., Wassenberg, Germany). The oven was preheated to 180 °C, and a temperature ramp up to 200 °C was initiated during the roasting process. Temperature measurements were conducted inside the roasting chamber as well as on the exhausted airflow. A total of four real-time roasts, each lasting 20 min, were monitored. The probe head (1 in Figure 3) was securely affixed with a mounting apparatus (2) to the drum roaster (4), positioned in front of the inspection glass (3) to observe the coffee beans (5). The working distance (d) between the coaxial probe and the inside of the drum roaster (4) was maintained at 35 mm. Measurements were taken every second, with an integration time of 10 ms.

(**a**)                                                                 (**b**)
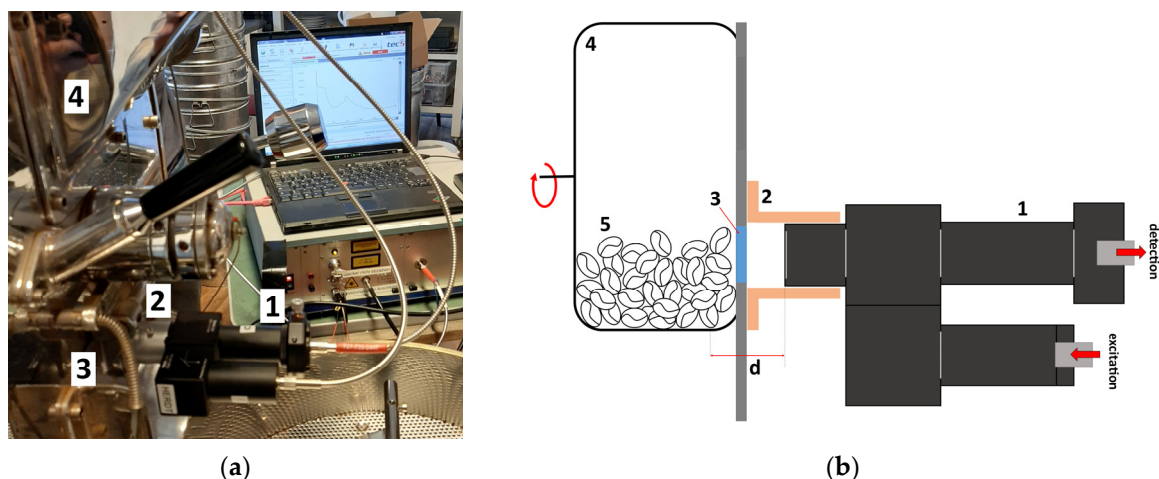
**Figure 3.** (**a**) Real-time roasting and (**b**) schematic representation of the experimental setup with the probe head (1), mounting apparatus (2), inspection glass (3), drum roaster (4) with rotating chamber (see arrow), coffee beans (5), and working distance (d).

*2.3. Spectroscopic Setup*

For spectroscopic analysis, the Multispec Raman spectrometer (tec5 AG, Steinbach, Germany) was used. It featured a monochromatic laser with an excitation wavelength of 785 nm and a nominal power of 300 mW. The optical range spanned from 320 to 3200 cm$^{-1}$, with an optical resolution of 5 cm$^{-1}$. The laser was integrated with an fiber-optic connector/physical contact (FC/PC) coupler into the probe head using a 100 µm core size optical fiber (Ocean Insight, Ostfildern, Germany). The laser beam underwent parallelization through the first plano-convex lens (f = 30 mm, Thorlabs GmbH, Bergkirchen, Germany) before incidence on the planar surface for collimation prior to passing through the bandpass filter (AHF Analysentechnik AG, Tübingen, Germany). Subsequently, the laser beam was deflected from the laser beam splitter (AHF Analysentechnik AG, Tübingen, Germany) into the second plano-convex lens (Thorlabs GmbH, Bergkirchen, Germany), which focused the light onto the sample with a focal length of 35 mm. Considering losses in coupling and due to the beam splitter, the power output of the probe head at the focal point was 80 mW. The inelastic scattered light from the sample was captured and parallelized by the plano-convex lens. The collimated signal of the light, transmitted through the beam splitter, was focused by the subsequent lens onto an optical fiber. The choice of optical fiber transmitting the detection signal to the spectrometer depended on the tested sample. A fiber patch cable with a 550 µm core (Thorlabs GmbH, Bergkirchen, Germany) was utilized for reference roastings, while a 600 µm optical fiber (Ocean Insight, Ostfildern, Germany) was connected to the spectrometer for real-time measurements.

*2.4. HPLC—(High-Pressure Liquid Chromatography) with Diode Array Detector Method for Determination of CGA*

To prepare the coffee samples for acid profile analysis, roasted coffee beans were freshly ground using the Krups Burr Grinder (Art.no.GVX242, Frankfurt am Main, Germany) immediately prior to extraction. For each extraction, 40 g of the ground coffee beans were combined with 400 milliliters of double-distilled water heated to 98 °C. The mixture was stirred every 2 min and maintained at 98 °C for 10 min. Following extraction, the coffee extracts were adjusted to their initial weight using double-distilled water, then filtered to remove any particulate matter. Subsequently, the filtered extracts were cooled and frozen until HPLC analysis. The acid profile qualification and quantification were conducted post-filtration using a 0.45 µm cellulose acetate membrane. Separation was achieved using a C18 column (OTU Lipomare C18, dimensions: 250 mm × 4.6 mm) and an additional precolumn (dimensions: 10 mm × 4.6 mm) from AppliChrom (Oranienburg, Germany). The solvent gradient consisted of eluent A (2% acetate in $H_2O$) and eluent B (2% acetate

in methanol). The measurement duration was 87 min, with specific gradients outlined in Table 2.

**Table 2.** HPLC-DAD gradient for quantitative analysis of CGA.

| Time (min) | Eluent A (%) | Eluent B (%) |
|:---:|:---:|:---:|
| 0.0 | 100 | 0 |
| 15.0 | 100 | 0 |
| 15.5 | 95 | 5 |
| 29.0 | 90 | 10 |
| 39.0 | 90 | 10 |
| 60.0 | 65 | 35 |
| 60.5 | 40 | 60 |
| 76.0 | 5 | 95 |
| 81.0 | 5 | 95 |
| 81.5 | 100 | 0 |
| 87.0 | 100 | 0 |

The mobile-phase flow rate used to determine the acid profile was set at 1 mL min$^{-1}$. Calibration was conducted using three different concentrations of a seven-acid standard mix (refer to Figure 4: caffeic, syringic, chlorogenic, p-coumaric, ferulic, sinapic, and cinnamic acid). Each injection consisted of 20 µL of either the standard mix or sample. The column oven temperature was maintained at 40 °C throughout the analysis. Detection and quantification were carried out using a diode array detector at wavelengths of 325 nm and 280 nm.
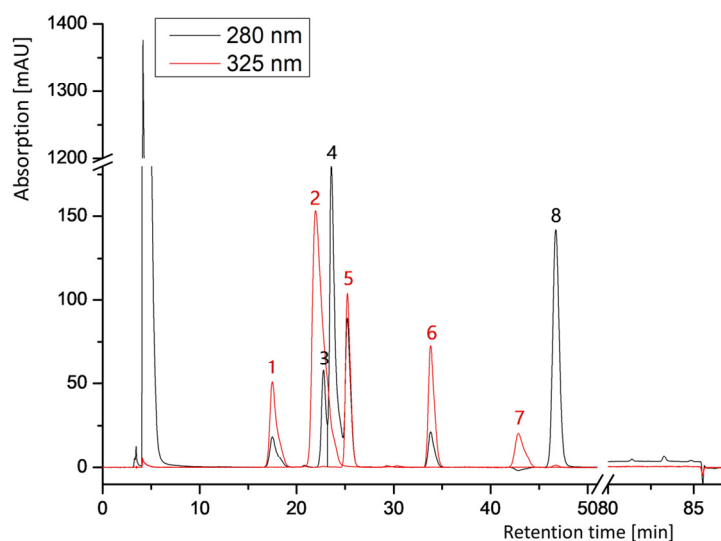


**Figure 4.** HPLC- DAD example chromatogram with acid mix containing 1 caffeic, 2 chlorogenic, 3 syringic, 4 coffein, 5 p-coumaric, 6 ferulic, 7 sinapic, and 8 cinnamic acid. Acid 3, 4, and 8 were measured at 280 nm, while the remaining acids were measured at 325 nm.

### 2.5. Sample Analysis

The roasted coffee beans, derived from roastings conducted in the laboratory fluidized bed roaster, underwent measurement to establish a calibration for assessing roasting progress in the laboratory. Each matrix value resulted from a fivefold measurement and was presented as the mean value. Spectral analysis identified molecule-selective regions highly responsive to roasting, contrasted against less sensitive regions. The analysis revealed discernible changes primarily between 500 cm$^{-1}$ and 1000 cm$^{-1}$. Regions beyond 2000 cm$^{-1}$ to 3200 cm$^{-1}$ exhibited minimal alterations and were therefore excluded from subsequent analyses. Consequently, datasets were confined to the range of 400 cm$^{-1}$ to 2000 cm$^{-1}$. The minimum (*min*) and maximum (*max*) values across the entire range were

determined and then divided for each measurement to serve as references. Thus, the constant $K^r$ ($r$ = reference) was calculated for each roasting temperature ($\vartheta$) relative to roasting time ($t$) as follows:

$$K^r_{\vartheta_n t_m} = \frac{max(I_{\vartheta_n t_m})^{2000}_{400}}{min(I_{\vartheta_n t_m})^{2000}_{400}} \tag{1}$$

with $n$ = 140 °C, 160 °C, 180 °C, and 200 °C and $m$ = 0, 180, 240, 300 . . . 3000 s.

The resultant matrix is displayed in Table 3.

**Table 3.** Matrix of $K^r$ constants for coffee roasting.

| | Roasting Temperature $\vartheta$ (°C) | | | |
|---|---|---|---|---|
| Roasting time $t$ (s) | 140 | 160 | 180 | 200 |
| 0 | | $\begin{bmatrix} K^r_{\vartheta 140 t0} \end{bmatrix}$ | $\cdots$ | $K^r_{\vartheta 200 t0}$ |
| . . . | | $\vdots$ | $\ddots$ | $\vdots$ |
| 3000 | | $K^r_{\vartheta 140 t3000}$ | $\cdots$ | $K^r_{\vartheta 200 t11620}$ |

For online measurements conducted in the drum roaster, the $K^o$ ($o$ = online) value was likewise computed using Formula (1) for each measurement, representing one recorded value every 100 ms. Given that the signals exhibited variations attributable to the different measurement setups, resulting in distinct constants, a deviation in the signal was observed, largely due to differences in the glass and general setups. To ascertain the correction factor A, the CGA concentration $c_{(0)}$ = 472 mg L$^{-1}$ was compared against the constants derived from both reference and online measurements of the unroasted beans in the roaster (initial roasting measurements devoid of temperature influence), as outlined below:

$$A = \frac{K^o_{\vartheta_0 t_0}}{K^r_{\vartheta_0 t_0}} = \frac{25.08}{8.57} = 2.93 \tag{2}$$

With the incorporation of this correction factor, the concentration of CGA, denoted as $c$, could be forecasted based on the roasting progress by applying the correction factor A to the $K^o$ value of each measurement using the following formula:

$$c_{\vartheta_n t_m} = A \cdot K^o_{\vartheta_n t_m} \tag{3}$$

Twenty Raman spectra were utilized for each second to compute a moving average to calculate the quotient $K^o$. Subsequently, this value was employed to estimate the theoretical concentrations of CGA.

Following this, the calculation of the deviations of the measured values from the theoretically calculated values, known as residual analysis, was performed. These deviations, referred to as residuals ($r$), are computed using the formula:

$$r = c_{HPLC} - c_{\vartheta_n t_m} \tag{4}$$

where $c_{HPLC}$ represents the measured CGA concentration by HPLC-DAD and $c_{\vartheta_n t_m}$ represents the predicted CGA concentrations.

The residuals were then utilized to assess the goodness of fit of the model. A metric for evaluating this quality is the Root Mean Squared Error (*RMSE*), which was calculated using the following formula:

$$RMSE = \sqrt{\frac{1}{n}\sum_{i=1}^{n}\left(c_{\vartheta_n t_m} - c_p\right)^2} \tag{5}$$

The *RMSE* provides a single measure of predictive accuracy, summarizing the average magnitude of the residuals and thus offering insights into the model's overall performance

in predicting the dependent variable. By incorporating residual analysis and calculating the RMSE, we can effectively quantify the discrepancy between the predicted and observed values, thereby providing an assessment of the model's predictive accuracy and reliability.

## 3. Results

In the following section, the results of the spectroscopic measurements and the subsequent analysis are shown.

### 3.1. Reference Measurement Roasting

The reference roasting conducted at 140 °C exhibited a progressively increasing signal with prolonged roasting time until reaching peak intensity at 2700 s. Conversely, the roasting series at 160 °C demonstrated its peak at 900 s, as depicted in Figure 5, illustrating the typical progression of the reference measurement at 160 °C across sampling times. To facilitate the assignment of individual sample times to their corresponding spectra, the times in the legend were organized in descending order of signal intensity in Figure 5.
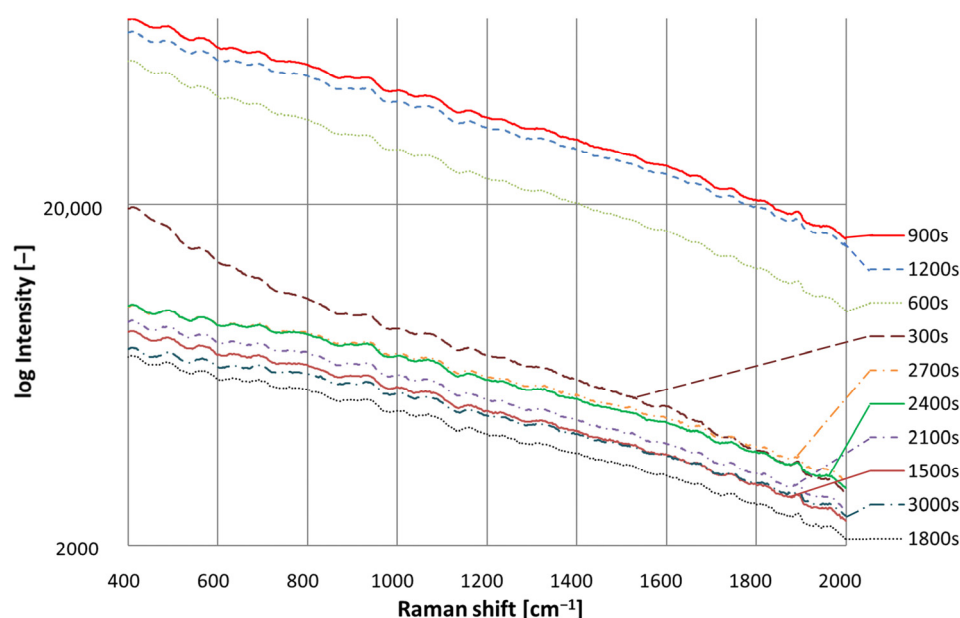


**Figure 5.** Spectroscopic progression of 160 °C samples across various sampling times.

At 180 °C, the maximum was attained by 720 s, while the series at 200 °C reached its peak at 360 s.

### 3.2. Online Roasting Measurement

Due to the spectroscopic setup, a spectrum was obtained every second during the roasting process. An average spectrum was computed due to better visibility for each minute, as illustrated in Figure 6, which depicts an exemplary roasting in the drum roaster lasting 21 min. To facilitate the assignment of individual roasting times to their corresponding mean value spectra in Figure 6, the legend times were arranged in descending order of signal intensity and a logarithmic scale was applied to the *y*-axis. Initially, the spectrum exhibits increasing intensity values across the entire range until the 19th minute. Subsequently, after reaching maximum intensity, the spectrum undergoes a significant decline, returning almost to the baseline level observed at the beginning of the roasting. This behavior was consistently observed across all four roasting processes, with the peak intensity occurring consistently between 18 and 19 min into the roasting process. Owing to the experimental setup, the spectra exhibit variability from one second to the next in intensity. This reflects the probe's measurement of the outer shell of coffee beans in different stages of roasting and varying compositions.
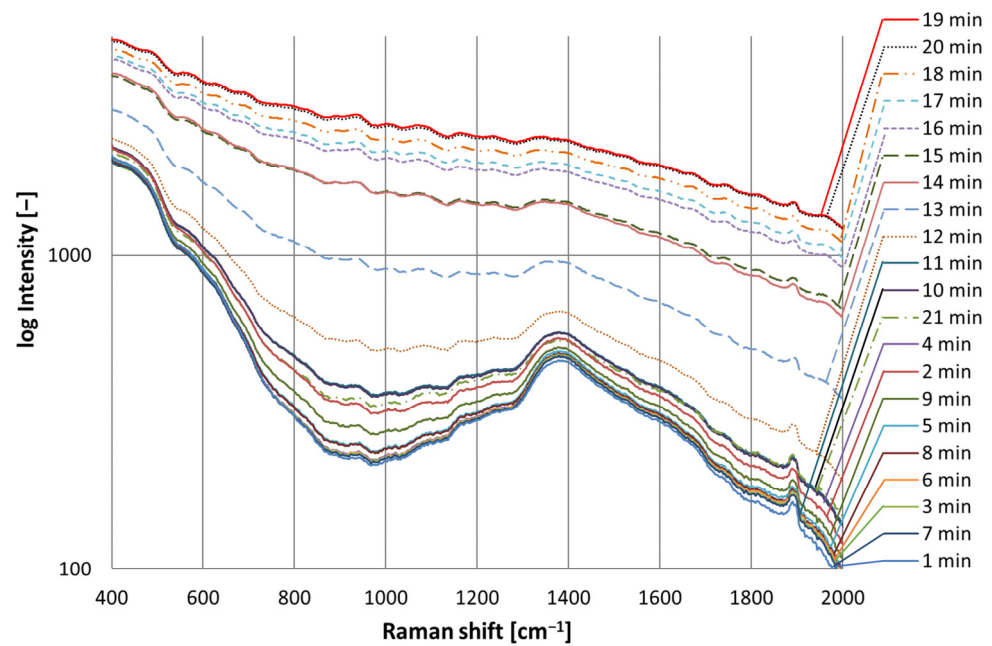
**Figure 6.** Mean value spectra of a typical online roasting with 21 min duration. One average spectrum was computed from 60 spectra for each minute.

### 3.3. HPLC-DAD Method for Determination of CGA

Table 4 presents the chlorogenic acid concentrations measured in roasted coffee beans at varying roasting temperatures and times using the HPLC-DAD method, along with the corresponding standard deviations ($\sigma$) calculated for each condition.

**Table 4.** Resulting reference roasting CGA concentrations from HPLC with calculated standard deviation ($\sigma$).

|  | 200 °C | $\sigma$ | 180 °C | $\sigma$ | 160 °C | $\sigma$ | 140 °C | $\sigma$ |
|---|---|---|---|---|---|---|---|---|
| 0 | 472 | 15.5 | 472 | 15.5 | 472 | 15.5 | 472 | 15.5 |
| 180 | 310 | 0.3 |  |  |  |  |  |  |
| 240 |  |  | 351 | 2.0 |  |  |  |  |
| 300 |  |  |  |  | 411 | 10.1 | 443 | 7.0 |
| 360 | 213 | 1.5 |  |  |  |  |  |  |
| 480 |  |  | 280 | 13.3 |  |  |  |  |
| 540 | 169 | 0.6 |  |  |  |  |  |  |
| 600 |  |  |  |  | 352 | 0.7 |  |  |
| 720 | 130 | 0.2 | 233 | 10.1 |  |  |  |  |
| 900 | 108 | 0.5 |  |  | 312 | 0.9 | 421 | 15.0 |
| 960 |  |  | 198 | 6.2 |  |  |  |  |
| 1200 |  |  | 176 | 1.0 | 297 | 0.6 | 405 | 11.0 |
| 1260 | 77 | 1.2 |  |  |  |  |  |  |
| 1440 | 65 | 1.6 | 157 | 0.4 |  |  |  |  |
| 1500 |  |  |  |  | 286 | 7.8 | 394 | 4.3 |
| 1620 | 63 | 1.0 |  |  |  |  |  |  |
| 1680 |  |  | 148 | 0.5 |  |  |  |  |
| 1800 |  |  |  |  |  |  | 376 | 2.5 |
| 1920 |  |  | 138 | 2.2 |  |  |  |  |
| 2100 |  |  |  |  | 266 | 8.9 | 374 | 3.5 |
| 2160 |  |  | 130 | 1.5 |  |  |  |  |
| 2400 |  |  | 101 | 0.1 | 254 | 14.1 | 364 | 3.5 |
| 2700 |  |  |  |  | 235 | 6.4 | 358 | 0.5 |
| 3000 |  |  |  |  | 220 | 0.3 | 355 | 0.1 |

The reference HPLC method revealed the time-dependent degradation of CGA, with an initial concentration of 472 mg $L^{-1}$. At 140 °C, the reference roasting indicated a reduction to 355 mg $L^{-1}$ by the end of the process, representing nearly one fourth of the initial concentration. By 600 s into the roasting at 160 °C, a similar degree of decomposition was observed (352 mg $L^{-1}$) and, after 3000 s, less than 50% of the initial CGA concentration remained (220 mg $L^{-1}$). At 180 °C and 200 °C, the concentrations decreased to 101 mg $L^{-1}$ and 63 mg $L^{-1}$, respectively. Generally, higher temperatures led to faster degradation of CGA, as depicted in Figure 7. The decomposition rate of CGA was more rapid in the early stages of roasting compared to later stages.
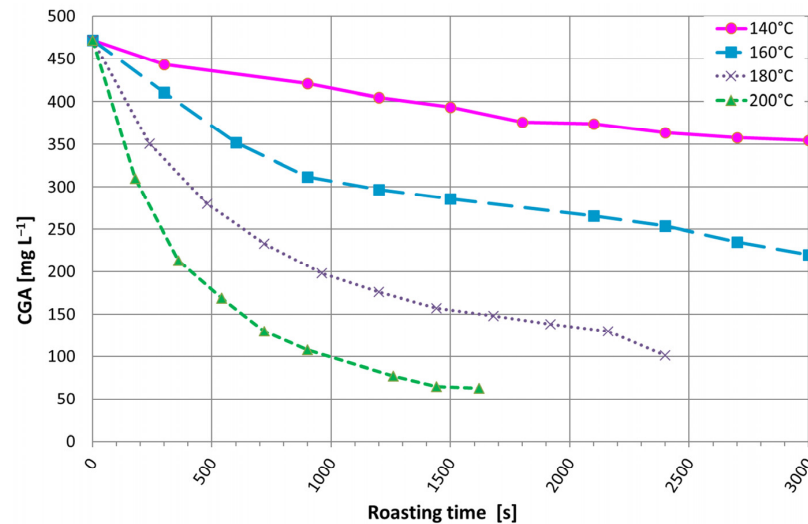


**Figure 7.** CGA concentration of roasted coffee beans over time.

### 3.4. Sample Analysis

The analysis of roasted samples revealed a progressive decrease in the quotient $K^r$ over time in the reference measurements. Initially, there was a noticeable descending trend, followed by a stabilization phase characterized by a minimum $K^r$ value that persisted until the end of the roasting process. This trend was particularly evident in the trials conducted at 180 °C and 200 °C. Similarly, for the measurements carried out at 140 °C and 160 °C, an initial descending trend was observed. Figure 8 illustrates the variations in the $K^r$ quotients for roasting temperatures ($\vartheta$) plotted against roasting time ($t$).
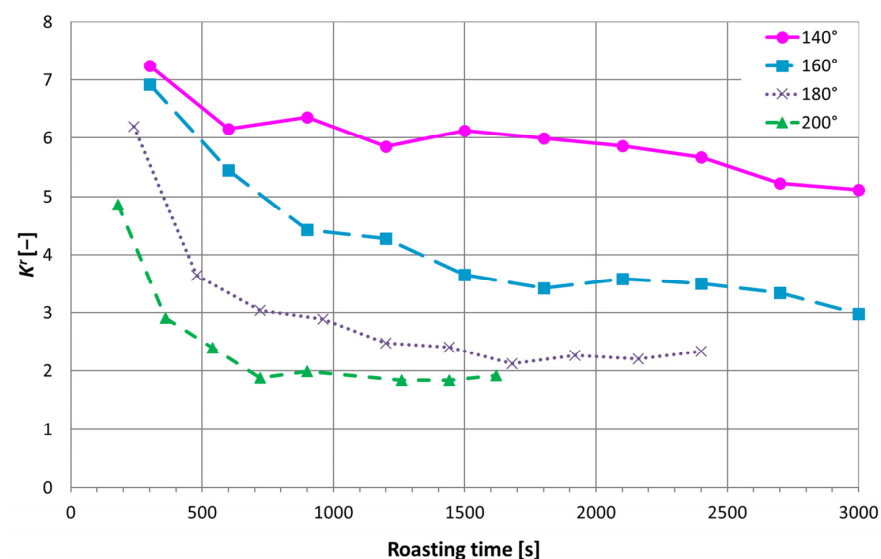


**Figure 8.** Progression of quotient $K^r$ for various temperatures across roasting time.

The quotient of the Raman signal $K^r$ and the concentration of CGA demonstrated a positive correlation, as depicted in Figure 9. This linear relationship yielded a coefficient of determination ($R^2$) of 0.9361, computed using the following formula:

$$c_{\vartheta_n t_m} = 65.00 \cdot K^r + 0.43 \tag{6}$$
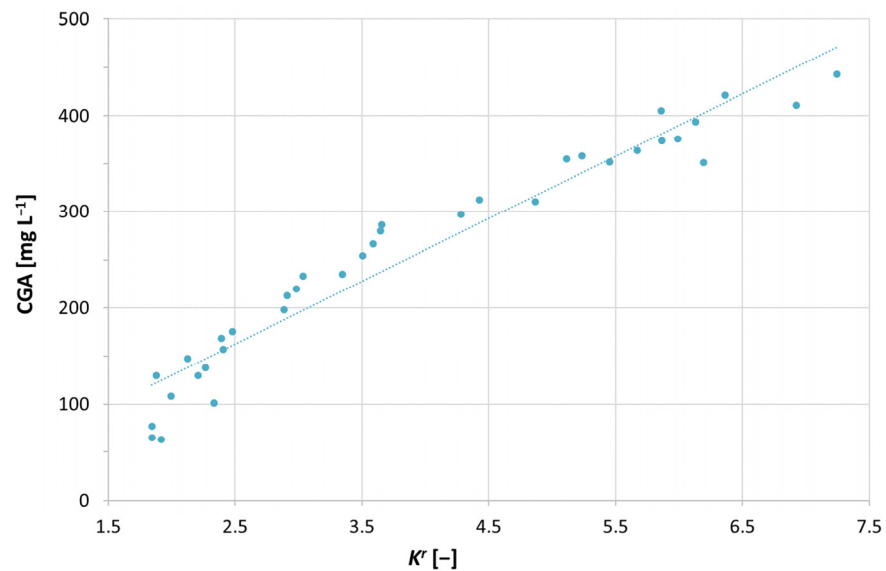


**Figure 9.** Linear correlation between $K^r$ and CGA concentration.

The calculated $K^r$ values from Equation (1), the measured CGA concentrations, the predicted CGA concentrations (Equation (3)), and their respective residuals (Equation (4)) are presented in Table 5. This illustrates the accuracy of the linear model in predicting CGA concentrations by highlighting the deviations between the measured and predicted values. The RMSE value further quantifies the model's predictive performance, indicating the average magnitude of residual errors in the CGA concentration predictions. It was determined to be 29.84 mg L$^{-1}$.

**Table 5.** $K^r$ values with corresponding roasting temperature, time, measured CGA concentration ($c_{HPLC}$), predicted CGA concentration ($c_{\vartheta_n t_m}$), and residual ($r$).

| $\vartheta$/°C | Time $t$/s | $K^r$/− | $c_{HPLC}$/g L$^{-1}$ | $c_{\vartheta_n t_m}$/g L$^{-1}$ | $r$/g L$^{-1}$ |
|---|---|---|---|---|---|
| 140 | 300 | 7.25 | 443.00 | 471.42 | −28.42 |
| | 900 | 6.36 | 421.00 | 414.03 | −6.97 |
| | 1200 | 5.86 | 405.00 | 381.25 | −23.75 |
| | 1500 | 6.13 | 394.00 | 398.86 | 4.86 |
| | 1800 | 5.99 | 376.00 | 389.85 | 13.85 |
| | 2100 | 5.86 | 374.00 | 381.58 | 7.58 |
| | 2400 | 5.67 | 364.00 | 369.04 | 5.04 |
| | 2700 | 5.23 | 358.00 | 340.55 | −17.45 |
| | 3000 | 5.11 | 355.00 | 332.89 | −22.11 |
| 160 | 300 | 6.92 | 411.00 | 450.46 | 39.46 |
| | 600 | 5.45 | 352.00 | 354.68 | 2.68 |
| | 900 | 4.43 | 312.00 | 288.19 | −23.81 |
| | 1200 | 4.28 | 297.00 | 278.56 | −18.44 |
| | 1500 | 3.66 | 286.00 | 238.12 | −47.88 |
| | 2100 | 3.59 | 266.00 | 233.64 | −32.36 |
| | 2400 | 3.51 | 254.00 | 228.41 | −25.59 |
| | 2700 | 3.34 | 235.00 | 217.76 | −17.24 |
| | 3000 | 2.98 | 220.00 | 194.18 | −25.82 |

**Table 5.** *Cont.*

| $\vartheta/°C$ | Time $t$/s | $K^r/-$ | $c_{HPLC}/g\ L^{-1}$ | $c_{\vartheta_n t_m}/g\ L^{-1}$ | $r/g\ L^{-1}$ |
|---|---|---|---|---|---|
| 180 | 240 | 6.19 | 351.00 | 402.90 | 51.90 |
| | 480 | 3.64 | 280.00 | 237.29 | −42.71 |
| | 720 | 3.04 | 233.00 | 197.77 | −35.23 |
| | 960 | 2.89 | 198.00 | 188.05 | −9.95 |
| | 1200 | 2.48 | 176.00 | 161.45 | −14.55 |
| | 1440 | 2.41 | 157.00 | 156.80 | −0.20 |
| | 1680 | 2.13 | 148.00 | 138.59 | −9.41 |
| | 1920 | 2.26 | 138.00 | 147.60 | 9.60 |
| | 2160 | 2.21 | 130.00 | 143.80 | 13.80 |
| | 2400 | 2.33 | 101.00 | 152.10 | 51.10 |
| 200 | 180 | 4.87 | 310.00 | 316.67 | 6.67 |
| | 360 | 2.91 | 213.00 | 189.43 | −23.57 |
| | 540 | 2.39 | 169.00 | 155.80 | −13.20 |
| | 720 | 1.88 | 130.00 | 122.57 | −7.43 |
| | 900 | 1.99 | 108.00 | 130.08 | 22.08 |
| | 1260 | 1.84 | 77.00 | 120.27 | 43.27 |
| | 1440 | 1.84 | 65.00 | 120.23 | 55.23 |
| | 1620 | 1.92 | 63.00 | 125.08 | 62.08 |
| | 1620 | 1.92 | 63.00 | 125.08 | 62.08 |

The linear correlation extends to the online measurements with the correction factor $A = 2.93$. Subsequently, the $K^o$ values are employed to compute theoretical CGA concentrations during roasting, as illustrated in Figure 10. For enhanced clarity, Figure 10 illustrates the moving average of 10 calculated values from Equation (3). The initial CGA concentration stood at 472 mg $L^{-1}$, while the final concentration of the Columbia coffee variety was 123 mg $L^{-1}$. In the initial phase, the concentration of CGA remains relatively stable until it initiates degradation after 8–10 min of roasting.
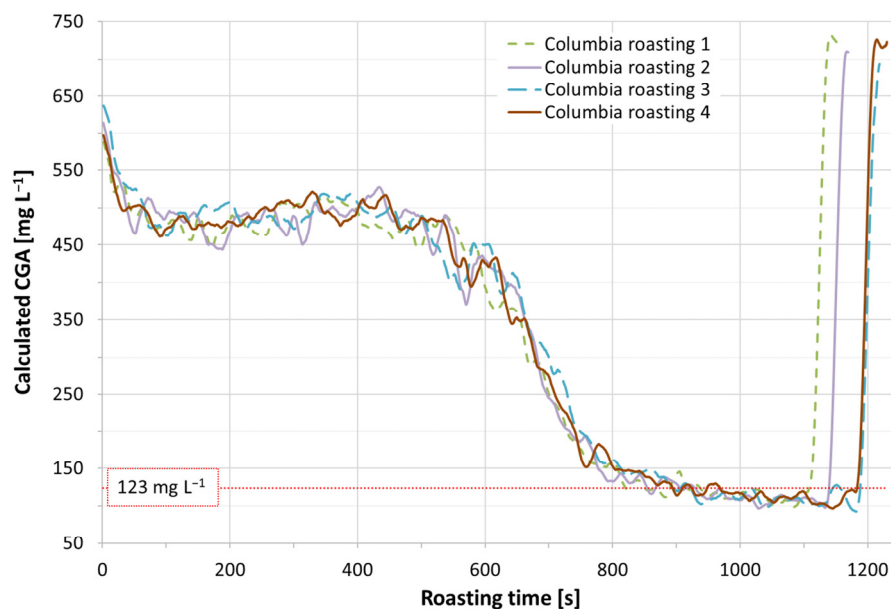


**Figure 10.** Theoretical CGA concentration profiles with moving average of four online roasting batches over time, with a final concentration of 123 mg $L^{-1}$ at the end point. Each batch consisted of 500 g of green coffee, roasted in a preheated oven at 180 °C with a temperature ramp up to 200 °C.

## 4. Discussion

The reference roasting series demonstrated a progressive increase in signal intensity as roasting time extended, achieving peak intensity at each of the four temperatures examined.

Higher temperatures resulted in a more rapid attainment of maximum signal intensity. This observation is consistent with Dias's [52] findings, where roasted and ground coffee exhibited an increase in the Raman response with decreasing wavenumber at 1064 nm excitation, indicative of fluorescence interference in dark samples. Following the peak, the spectrum intensity gradually declined with each sampling interval until the conclusion. This decline may be attributed to chemical transformations, resulting in the generation of fluorescent intermediates and end products up to a certain threshold.

Throughout the roasting process, these reactions occur uniformly within the entire coffee bean. Over time, as the beans undergo roasting, chemical compounds degrade, leading to a reduction in fluorescent signal intensity. The homogeneous heat distribution in the laboratory fluidized bed roaster ensures nearly uniform roasting of coffee beans.

Although a comprehensive evaluation of various roasting methods is beyond the scope of this paper, it is essential to consider the type of heat input and its impact on the homogeneity of the roasted product when applying this method to alternative roasting techniques. The fundamentally different power transfers in fluidized bed roasters and contact roasters, like a drum roaster, must be taken into account. Future studies should address these specific effects. Moreover, the noncontact method with short measurement times offers a novel approach to investigating the homogeneity of the roasted product during the roasting process for the first time. This technique could significantly enhance our understanding and control of roasting homogeneity in several roaster types.

A significant limitation of this study is its focus on a single coffee variety, which may not yield insights that are applicable across other coffee varieties than the Columbia Excelso variety. Different varieties can exhibit considerable variation in their chemical composition and their behavior during the roasting process [53].

Moreover, while chlorogenic acid is a crucial compound, an exclusive focus on it may overlook other significant compounds that play vital roles in flavor development through the Maillard reaction and Strecker degradation [11,20,22,54]. This narrow scope could potentially limit the understanding of the full spectrum of chemical changes occurring during coffee roasting.

Additionally, since the samples were milled before spectroscopic measurement, these changes were readily observable in the reference measurement of inelastic light scattering. The discrepancy in measurement conditions between offline (milled samples) and online (whole coffee bean) setups may introduce inconsistencies and affect the accuracy of the spectroscopic data. Four online measurements of the coffee bean roasting process were conducted, focusing solely on the outer shell of the beans. After 18 or 19 min, a decline in signal intensity was observed across the entire spectrum. Unlike the reference setup, where the entire roasted bean was ground before spectroscopic measurement, the online measurements utilized whole coffee beans in a rotating drum roaster with nonuniform heat distribution. This setup differed from the reference trials, which employed a fluidized bed chamber with more uniform temperature distribution.

To address these limitations, future research should include multiple coffee varieties to validate and generalize findings across different chemical profiles and roasting behaviors. Investigating diverse roasting methods, such as drum roasting and fluid bed roasting, which are used mainly in the coffee industry, will provide a comprehensive understanding of their impact on the Maillard reaction and Strecker degradation.

Investigating diverse coffee roasting methods, such as drum roasting and fluid bed roasting, which are predominantly used in the coffee industry, will provide a comprehensive understanding of their impact on the Maillard reaction and Strecker degradation. These methods influence the thermal environment and, consequently, the chemical reactions that develop desirable coffee flavor compounds. Expanding chemical analysis to include those compounds beyond CGA will offer a more holistic view of chemical transformations during roasting. Implementing these recommendations will refine the methodology and broaden its applicability, leading to a deeper understanding of coffee chemistry and optimized roasting processes. This approach ensures a thorough analysis of flavor development,

considering the crucial chemical changes during roasting that affect coffee quality and sensory characteristics.

The online roasting setup involved a rotating chamber over a gas flame, where heat transfer occurred conductively through contact between the beans and the hot stainless-steel wall. Consequently, some beans did not directly contact the hot wall, leading to slower heat transfer and nonuniform roasting of individual beans. The variability in the Raman spectra due to nonuniform roasting in the online setup highlights the importance of considering the inherent heterogeneity of coffee beans. Studies have shown that Raman spectra differ across various spots and regions within the green coffee bean structure, likely due to the three-dimensional inhomogeneity in the chemical composition and structure of the green beans [50,51]. This phenomenon is also anticipated in roasted coffee beans, where the uneven chemical composition leads to different reactions during roasting [50]. Additionally, online roasting required more time to exhibit both the initial increase and subsequent decline in signal intensity compared to reference roasting, indicating slower chemical changes within the coffee beans. Throughout the roasting process, coffee beans release moisture and carbon dioxide, a phenomenon crucial for developing roast flavors and achieving the characteristic brown color of roasted coffee beans. Subsequent to the first crack, volatile aroma compounds undergo further transformation via esterification, oxidation, and pyrolysis, significantly enhancing the aromatic profile of coffee. These reactions may contribute to the rapid decomposition of CGA observed during online roasting. Luna et al. [50] employed Raman spectroscopy to classify clonal varieties of green coffee. The study identified prominent peaks at approximately $1600 \text{ cm}^{-1}$ and $1630 \text{ cm}^{-1}$, which were attributed to phenyl ring stretch and C=C stretch vibrations, respectively. Additionally, weaker peaks were observed around $1120 \text{ cm}^{-1}$ and $1200 \text{ cm}^{-1}$, corresponding to CH, COH bending, and phenyl ring bending vibrations. These spectral features are consistent with the presence of chlorogenic acids (CGA), lipids, and proteins, all of which are involved in several reactions during the roasting process. However, these changes may not always manifest visibly in the outer shell spectrum. Monitoring the outer shell during online roasting has proven sensitive to bean composition variations, resulting in observable color shifts and chemical mixtures. Such discrepancies arise from uneven heat distribution within the roaster and the beans themselves, complicating the monitoring process. Initially, the CGA concentration was $472 \text{ mg L}^{-1}$ and, as expected, it decreased for all reference roasting temperature sets. In the beginning, the degradation rate was higher than towards the end for all four temperatures [21]. However, for the 200 °C roasting, the last two samples exhibited nearly identical concentrations at $65 \text{ mg L}^{-1}$ and $63 \text{ mg L}^{-1}$, indicating minimal change within 180 s. This contrasted with the initial breakdown of CGA, which exceeded 30% within the same timeframe. Concentrations during online roasting could not be determined due to the absence of samples, which could lead to a drop in temperature in the roasting chamber. However, the final concentration of $123 \text{ mg L}^{-1}$ closely resembled the two final values of the 180 °C roasting series in the reference setup: $138 \text{ mg L}^{-1}$ at 1920 s and $130 \text{ mg L}^{-1}$ at 2160 s. Considering that the online measurement in the roaster also commenced at 180 °C and the beans heated up to 200 °C over approximately 20 min, similar concentrations were anticipated.

However, it is important to note that sampling during the roasting process presented various challenges. Even minimal temperature drops due to sampling could potentially distort the roasting time and degree of the remaining coffee beans in the roasting chamber. Therefore, no additional samples were taken between the green coffee bean stage and the final roasted stage. Future research should investigate how the effects of decreasing roasted goods due to sampled volume in the roasting chamber and temperature drops impact the overall roasting time.

The analysis of roasted samples revealed a decreasing quotient $K^r$ over time for the reference measurements. Initially, there was a descending trend, followed by a minimum value of $K^r$, which remained almost constant towards the end. This trend was notably observed for the reference roasting temperatures of 180 °C and 200 °C. While the descending

trend was also apparent for the 140 °C and 160 °C measurements, the plateau was not as explicitly observed. Without further samples, it was unclear whether the value would exhibit a declining trend or stabilize on a plateau. With higher temperatures, the chemical changes during roasting progressed more rapidly, leading to an observable endpoint in the spectroscopic measurements. This phenomenon might be attributed to the darker color observed towards the end of the roasting process. As the coffee beans underwent further roasting, chemical compounds were increasingly destroyed, resulting in a decrease in the fluorescent signal over time.

Fluorescence evaluation was found to simplify the analysis process by encompassing entire areas rather than focusing solely on specific Raman peaks. This approach streamlines signal acquisition, enhancing its stability and making the analysis more straightforward. The overarching goal is to establish a robust measurement technology that emphasizes efficiency and reliability in assessing coffee roasting progress. By embracing fluorescence and its broad evaluation capabilities, the methodology aims to enhance the overall robustness of the measurement process, ensuring accurate and dependable results across various analytical applications.

## 5. Conclusions

The findings suggest that employing inelastic light scattering measurement on a drum roaster holds promise for monitoring purposes. A correlation between the inelastic scattered light and CGA, a potential control parameter, was established. Through laboratory measurements conducted at fixed roasting temperatures and durations, a calibration matrix comprising calculated quotients was generated. These quotients were utilized to estimate theoretical CGA concentrations. This inference was validated through four live roastings, yielding a theoretical CGA concentration of approximately 123 mg L$^{-1}$ at the conclusion of the process, as depicted in Figure 10. The corresponding result from the HPLC measurement stood at 123 mg L$^{-1}$. For prospective applications, the measurement could serve as a calculated variable and termination criterion with a Raman photometer. By accurately monitoring the process using two Raman shift values, a robust photometer equipped with suitable band-pass filters could be developed. Single photon counters linked to photo sensory detectors within the desired wavelength ranges would be employed in this setup. This approach presents a cost-effective and verifiable alternative for real-time monitoring.

GmbH. The remaining authors declare that the research was conducted in the absence of any commercial or financial relationships that could be construed as a potential conflict of interest.

## References

1. Franca, A.S.; Mendonça, J.C.; Oliveira, S.D. Composition of green and roasted coffees of different cup qualities. *LWT-Food Sci. Technol.* **2005**, *38*, 709–715. [CrossRef]
2. Hernández, J.A.; Heyd, B.; Trystram, G. On-line assessment of brightness and surface kinetics during coffee roasting. *J. Food Eng.* **2008**, *87*, 314–322. [CrossRef]
3. Hernández, J.A.; Heyd, B.; Trystram, G. Prediction of brightness and surface area kinetics during coffee roasting. *J. Food Eng.* **2008**, *89*, 156–163. [CrossRef]
4. Winjaya, F.; Rivai, M.; Purwanto, D. Identification of cracking sound during coffee roasting using neural network. In Proceedings of the 2017 International Seminar on Intelligent Technology and Its Applications (ISITIA), Surabaya, Indonesia, 28–29 August 2017; IEEE: New York, NY, USA, 2017.
5. Wilson, P.S. Coffee roasting acoustics. *J. Acoust. Soc. Am.* **2014**, *135*, EL265–EL269. [CrossRef] [PubMed]
6. Corzo-Martínez, M.; Corzo, N.; Villamiel, M.; del Castillo, M.D. Browning Reactions. In *Food Biochemistry and Food Processing*, 2nd ed.; Simpson, B.K., Ed.; John Wiley & Sons: Hoboken, NJ, USA, 2012; pp. 56–83. ISBN 9780813808741.
7. Kroh, L.W. Caramelisation in food and beverages. *Food Chem.* **1994**, *51*, 373–379. [CrossRef]
8. Martins, S.I.; Jongen, W.M.; van Boekel, M.A. A review of Maillard reaction in food and implications to kinetic modelling. *Trends Food Sci. Technol.* **2000**, *11*, 364–373. [CrossRef]
9. Nursten, H.E. *The Maillard Reaction: Chemistry, Biochemistry and Implications*; Royal Society of Chemistry: Cambridge, UK, 2005; ISBN 978-0-85404-964-6.
10. Maillard, L.C. Action of amino acids on sugars. Formation of melanoidins in a methodical way. *Compte-Rendu L'Academie Sci.* **1912**, *154*, 66–68.
11. van Boekel, M.A.J.S. Formation of flavour compounds in the Maillard reaction. *Biotechnol. Adv.* **2006**, *24*, 230–233. [CrossRef]
12. van Boekel, M.A.J.S. Kinetic aspects of theMaillard reaction: A critical review. *Nahrung* **2001**, *45*, 150–159.
13. Mohsin, G.F.; Schmitt, F.-J.; Kanzler, C.; Dirk Epping, J.; Flemig, S.; Hornemann, A. Structural characterization of melanoidin formed from d-glucose and l-alanine at different temperatures applying FTIR, NMR, EPR, and MALDI-ToF-MS. *Food Chem.* **2018**, *245*, 761–767. [CrossRef]
14. Moon, J.-K.; Shibamoto, T. Formation of volatile chemicals from thermal degradation of less volatile coffee components: Quinic acid, caffeic acid, and chlorogenic acid. *J. Agric. Food Chem.* **2010**, *58*, 5465–5470. [CrossRef]
15. Strecker, A. Ueber die künstliche Bildung der Milchsäure und einen neuen, dem Glycocoll homologen Körper. *Justus Liebigs Ann. Der Chem.* **1850**, *75*, 27–45. [CrossRef]
16. Finot, P. *The Maillard Reaction in Food Processing, Human Nutrition and Physiology*; Birkhäuser: Basel, Switzerland; Boston, MA, USA; Berlin, Germany; Stuttgart, Germany, 1990; ISBN 9783764323547.
17. Belitz, H.-D.; Grosch, W.; Schieberle, P. *Food Chemistry*, 4th ed.; Springer: Berlin/Heidelberg, Germany, 2009; ISBN 978-3-540-69933-0.
18. Kanzler, C.; Schestkowa, H.; Haase, P.T.; Kroh, L.W. Formation of Reactive Intermediates, Color, and Antioxidant Activity in the Maillard Reaction of Maltose in Comparison to d-Glucose. *J. Agric. Food Chem.* **2017**, *65*, 8957–8965. [CrossRef]
19. Kunz, T.; Strähmel, A.; Cortés, N.; Kroh, L.W.; Methner, F.-J. Influence of Intermediate Maillard Reaction Products with Enediol Structure on the Oxidative Stability of Beverages. *J. Am. Soc. Brew. Chem.* **2013**, *71*, 114–123. [CrossRef]
20. Moon, J.-K.; Shibamoto, T. Role of Roasting Conditions in the Profile of Volatile Flavor Chemicals Formed from Coffee Beans. *J. Agric. Food Chem.* **2009**, *57*, 5823–5831. [CrossRef]
21. Rusinek, R.; Dobrzański, B., Jr.; Gawrysiak-Witulska, M.; Siger, A.; Żytek, A.; Karami, H.; Umar, A.; Lipa, T.; Gancarz, M. Effect of the roasting level on the content of bioactive and aromatic compounds in Arabica coffee beans. *Int. Agrophys.* **2023**, *38*, 31–42. [CrossRef] [PubMed]
22. Parker, J.K. *Flavour Development, Analysis and Perception in Food And Beverages*, 1st ed.; Elsevier Science: Burlington, MA, USA, 2014; ISBN 1-78242-111-4.
23. Moon, J.-K.; Yoo, H.S.; Shibamoto, T. Role of roasting conditions in the level of chlorogenic acid content in coffee beans: Correlation with coffee acidity. *J. Agric. Food Chem.* **2009**, *57*, 5365–5369. [CrossRef] [PubMed]
24. Awwad, S.; Issa, R.; Alnsour, L.; Albals, D.; Al-Momani, I. Quantification of Caffeine and Chlorogenic Acid in Green and Roasted Coffee Samples Using HPLC-DAD and Evaluation of the Effect of Degree of Roasting on Their Levels. *Molecules* **2021**, *26*, 7502. [CrossRef]
25. Trugo, L.C.; Macrae, R. A study of the effect of roasting on the chlorogenic acid composition of coffee using HPLC. *Food Chem.* **1984**, *15*, 219–227. [CrossRef]
26. Clarke, R.J. *Coffee: Recent Developments*; Blackwell: Oxford, UK, 2008; ISBN 0632055537.
27. Banks, M. *The Complete Book of Coffee: The Definitive Guide to Coffee, from Simple Bean to Irresistible Beverage*; Lorenz Books: London, UK, 2021; ISBN 9780754835554.
28. Fischer, C. *Kaffee: Änderung Physikalisch-Chemischer Parameter beim Rösten, Quenchen und Mahlen*, 1st ed.; Cuvillier Verlag: Göttingen, Germany, 2005; ISBN 3865374379.

29. Baggenstoss, J.; Poisson, L.; Kaegi, R.; Perren, R.; Escher, F. Coffee roasting and aroma formation: Application of different time-temperature conditions. *J. Agric. Food Chem.* **2008**, *56*, 5836–5846. [CrossRef]

30. Hoffmann, J. *The World Atlas of Coffee: From Beans to Brewing—Coffees Explored, Explained and Enjoyed*, 2nd ed.; Firefly Books: Buffalo, NY, USA, 2018; ISBN 0228100941.

31. Hii, C.L.; Borém, F.M. *Drying and Roasting of Cocoa and Coffee*; CRC Press: Boca Raton, FL, USA, 2020; ISBN 9781351624022.

32. Barbin, D.F.; Felicio, A.L.d.S.M.; Sun, D.-W.; Nixdorf, S.L.; Hirooka, E.Y. Application of infrared spectral techniques on quality and compositional attributes of coffee: An overview. *Food Res. Int.* **2014**, *61*, 23–32. [CrossRef]

33. Esteban-Díez, I.; González-Sáiz, J.M.; Pizarro, C. Prediction of Roasting Colour and other Quality Parameters of Roasted Coffee Samples by near Infrared Spectroscopy. A Feasibility Study. *J. Near Infrared Spectrosc.* **2004**, *12*, 287–297. [CrossRef]

34. Tolessa, K.; Rademaker, M.; de Baets, B.; Boeckx, P. Prediction of specialty coffee cup quality based on near infrared spectra of green coffee beans. *Talanta* **2016**, *150*, 367–374. [CrossRef] [PubMed]

35. Pizarro, C.; Esteban-Díez, I.; González-Sáiz, J.-M.; Forina, M. Use of near-infrared spectroscopy and feature selection techniques for predicting the caffeine content and roasting color in roasted coffees. *J. Agric. Food Chem.* **2007**, *55*, 7477–7488. [CrossRef] [PubMed]

36. Santos, J.R.; Viegas, O.; Páscoa, R.N.M.J.; Ferreira, I.M.P.L.V.O.; Rangel, A.O.S.S.; Lopes, J.A. In-line monitoring of the coffee roasting process with near infrared spectroscopy: Measurement of sucrose and colour. *Food Chem.* **2016**, *208*, 103–110. [CrossRef] [PubMed]

37. Alessandrini, L.; Romani, S.; Pinnavaia, G.; Dalla Rosa, M. Near infrared spectroscopy: An analytical tool to predict coffee roasting degree. *Anal. Chim. Acta* **2008**, *625*, 95–102. [CrossRef]

38. Grassi, S.; Giraudo, A.; Novara, C.; Cavallini, N.; Geobaldo, F.; Casiraghi, E.; Savorani, F. Monitoring Chemical Changes of Coffee Beans During Roasting Using Real-time NIR Spectroscopy and Chemometrics. *Food Anal. Methods* **2023**, *16*, 947–960. [CrossRef]

39. Pizarro, C.; Esteban-Díez, I.; Nistal, A.-J.; González-Sáiz, J.-M. Influence of data pre-processing on the quantitative determination of the ash content and lipids in roasted coffee by near infrared spectroscopy. *Anal. Chim. Acta* **2004**, *509*, 217–227. [CrossRef]

40. Suchánek, M.; Filipová, H.; Volka, K.; Delgadillo, I.; Davies, A.N. Qualitative analysis of green coffee by infrared spectrometry. *Anal. Bioanal. Chem.* **1996**, *354*, 327–332. [CrossRef]

41. Lyman, D.J.; Benck, R.; Dell, S.; Merle, S.; Murray-Wijelath, J. FTIR-ATR analysis of brewed coffee: Effect of roasting conditions. *J. Agric. Food Chem.* **2003**, *51*, 3268–3272. [CrossRef]

42. Reis, N.; Botelho, B.G.; Franca, A.S.; Oliveira, L.S. Simultaneous Detection of Multiple Adulterants in Ground Roasted Coffee by ATR-FTIR Spectroscopy and Data Fusion. *Food Anal. Methods* **2017**, *10*, 2700–2709. [CrossRef]

43. Ribiero, J.S.; SALVA, T.J.; FERREIRA, M.M. Chemometric Studies for Quality Control of Processed Brazilian Coffees using DRIFTS. *J. Food Qual.* **2010**, *33*, 212–227. [CrossRef]

44. Kemsley, E. Discrimination between Coffea arabica and Coffea canephora variant robusta beans using infrared spectroscopy. *Food Chem.* **1995**, *54*, 321–326. [CrossRef]

45. Munyendo, L.; Njoroge, D.; Hitzmann, B. The Potential of Spectroscopic Techniques in Coffee Analysis—A Review. *Processes* **2022**, *10*, 71. [CrossRef]

46. McCreery, R.L. *Calibration and Validation. Raman Spectroscopy for Chemical Analysis*; John Wiley & Sons: Hoboken, NJ, USA, 2005; pp. 251–291.

47. Hoffmann, G.G. *Infrared and Raman Spectroscopy: Principles and Applications*, 1st ed.; De Gruyter: Berlin, Germany; Boston, MA, USA, 2023; ISBN 9783110717556.

48. Rubayiza, A.B.; Meurens, M. Chemical discrimination of arabica and robusta coffees by Fourier transform Raman spectroscopy. *J. Agric. Food Chem.* **2005**, *53*, 4654–4659. [CrossRef] [PubMed]

49. Hu, Q.; Sellers, C.; Kwon, J.S.-I.; Wu, H.-J. Integration of surface-enhanced Raman spectroscopy (SERS) and machine learning tools for coffee beverage classification. *Digit. Chem. Eng.* **2022**, *3*, 100020. [CrossRef] [PubMed]

50. Luna, A.S.; Da Silva, A.P.; Da Silva, C.S.; Lima, I.C.; de Gois, J.S. Chemometric methods for classification of clonal varieties of green coffee using Raman spectroscopy and direct sample analysis. *J. Food Compos. Anal.* **2019**, *76*, 44–50. [CrossRef]

51. El-Abassy, R.M.; Donfack, P.; Materny, A. Discrimination between Arabica and Robusta green coffee using visible micro Raman spectroscopy and chemometric analysis. *Food Chem.* **2011**, *126*, 1443–1448. [CrossRef]

52. Dias, R.C.E.; Yeretzian, C. Investigating Coffee Samples by Raman Spectroscopy for Quality Control—Preliminary Study. *Int. J. Exp. Spectrosc. Tech.* **2016**, *1*, 1–5. [CrossRef]

53. Dippong, T.; Dan, M.; Kovacs, M.H.; Kovacs, E.D.; Levei, E.A.; Cadar, O. Analysis of Volatile Compounds, Composition, and Thermal Behavior of Coffee Beans According to Variety and Roasting Intensity. *Foods* **2022**, *11*, 3146. [CrossRef]

54. Kamiyama, M.; Moon, J.-K.; Jang, H.W.; Shibamoto, T. Role of degradation products of chlorogenic acid in the antioxidant activity of roasted coffee. *J. Agric. Food Chem.* **2015**, *63*, 1996–2005. [CrossRef] [PubMed]